Journal of the European Ceramic Society 21 (2001) 1625–1628

www.elsevier.com/locate/jeurceramsoc

Mechanisms for optical oscillations in ferroelectric films

R.A. O'Sullivan, [a,b,*], K.W. McGregor [a], O. Gredeskoul [a], J.F. Scott [b]

[a] *Department of Applied Physics, Royal Melbourne Institute of Technology, Box 2476V, GPO Melbourne, Victoria 3001, Australia*
[b] *Department of Earth Sciences, University of Cambridge, Cambridge CB2 3EQ, UK*

Received 4 September 2000; received in revised form 6 December 2000; accepted 10 December 2000

Abstract

Under steady laser illumination, aperiodic spatio-temporal oscillations are observed in the light transmitted and reflected by parallel-sided samples of the ferroelectrics PMN (lead magnesium niobate, $Pb(Mg_{1/3}Nb_{2/3})O_3$), PLZT (lanthanum doped lead zirconium titanate, $Pb(Zr_{1-x}Ti_x)O_3$:La), BNN (barium sodium niobate, $Ba_2NaNb_5O_{15}$) and Ce:SBN (cerium doped strontium barium niobate, Ce^{3+}:$Sr_xBa_{1-x}Nb_2O_6$). There are two distinct mechanisms for such oscillations, namely (1) unistable thermal focusing oscillations, which occur in BNN and Ce:SBN and (2) bistable or multistable Fabry-Perot switching oscillations, as observed in PMN and PLZT. The two types of oscillation have characteristic time scales differing by several orders of magnitude. We derive temperature profiles as a function of incident laser power, beamwidth and sample thickness, which quantitatively predict the spatio-temporal characteristics of the transmitted beam patterns. © 2001 Elsevier Science Ltd. All rights reserved.

Keywords: Ferroelectric properties; Optical properties; Perovskites; PLZT; Thermal properties

1. Introduction

The first observation of thermal focusing in a ferroelectric crystal was by Akhmanov et al.[1] in lithium niobate ($LiNbO_3$). This effect was later observed in ferroelectric ceramics.[2,11] More recently spontaneous aperiodic oscillations in the intensity and spatial structure of the output beams have been observed under steady laser illumination of PMN, PLZT, Ce:SBN and BNN.[3–6,18] In PMN the oscillations are smooth, with approximately equal rise and fall times, at low power but take the form of relaxation oscillations at higher power[14] cf. Fig. (1) Initial observations with PLZT also showed smooth oscillations [8,12,13] but we have recently observed the transition from smooth oscillations to relaxation oscillations at an incident power of about 0.7 W in a 1 mm ceramic PLZT sample. In BNN and Ce:SBN, on the other hand, only smooth oscillations have been observed, cf. Fig. (2) The oscillatory phenomena in the ferroelectrics PMN and PLZT have been explained qualitatively in terms of optical bistability (OB) arising from intrinsic Fabry-Perot resonance[7,12,15,20] and a quantitative fit has been made between the spatio-temporal temperature profile derived from this model and the real-time interferometrically measured temperature within a PMN crystal during relaxation oscillations of a transmitted Ar laser beam.[15]

Although the phenomena described here are intrinsically slow (ms) and hence of little interest for ns or ps photonic switching systems, they nevertheless provide several possible commercial applications: First is the their use as passive intra-cavity noise reduction devices for argon ion lasers,[17] where they cause beam divergence when the power level fluctuates upwards and beam convergence when it fluctuates downwards. Second is the use of the switching times of thermal relaxation oscillations to obtain direct information on the temperature dependence of thermal conductivity and thermo-optic coefficient of ferroelectrics near their phase transition. Third is the use of PMN thick films with readily available Ar^+ lasers for classroom demonstrations of optical bistability and regenerative pulsations. Fourth is their use as purely photonic sensors (no wires in or out) for air pressure and flow rate, due to the convective heat transfer at the sample surfaces, with a sensitivity of 0.1 Torr absolute pressure and the capability to measure flow rates as low as 0.003 m^3/h at 1 atm.[6]

* Corresponding author. Tel.: +613-9925-3389; fax: +613-9925-5290.

E-mail address: r.osullivan@rmit.edu.au (R.A. O'Sullivan).

PII: S0955-2219(01)00079-6

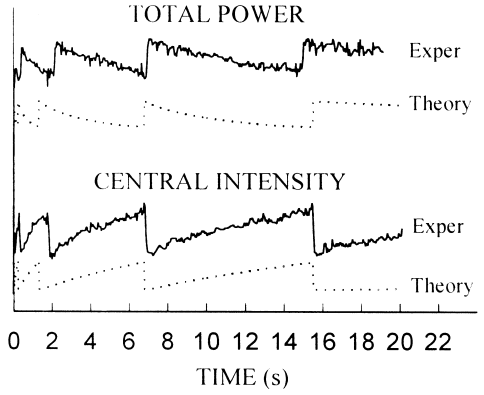

Fig. 1. Transmitted power (top) and central transmitted irradiance (bottom) for a 0.74 mm thick PMN single crystal following laser switch-on with $w = 28$ μm as measured experimentally (solid curves) and computed from the solution of Eqs. (1)–(7) (dotted curves).

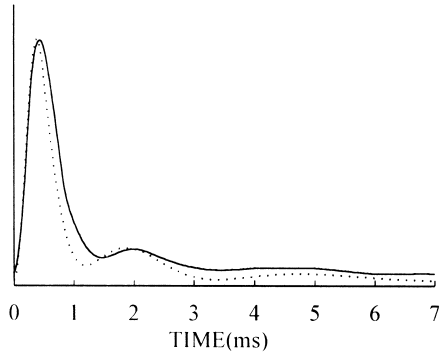

Fig. 2. Central intensity decay curves following laser switch-on to 61 mW for a 1.9 mm thick Ce^{3+}:$Sr_xBa_{1-x}Nb_2O_6$ (SBN) sample with $w = 190$ μm as given experimentally in Fig. 5 of Ref. 3 (solid curve) and computed from the solution of Eqs. (1)–(7) with a shutter time of 0.4 ms (dotted curve).

2. Theoretical model

The equations governing the system are the heat Eq. (1) coupled to Maxwell's equations for the forward and backward travelling light beams in the slowly varying envelope approximation (SVEA)[9,19] (2) and (3):

$$\nabla_u^2 T + (w/L)^2 \partial^2 T/\partial_\varsigma^2 - \partial T/\partial\tau = -\alpha_a w^2 I_c/K \tag{1}$$

$$\partial E_F/\partial\varsigma = -\frac{1}{2}\alpha L E_F + ikLn(T)E_F + i(\mathcal{F}/2)\nabla_u^2 E_F \tag{2}$$

$$\partial E_B/\partial\varsigma = \frac{1}{2}\alpha L E_B - ikLn(T)E_B - i(\mathcal{F}/2)\nabla_u^2 E_B \tag{3}$$

with the boundary conditions for the region $0 \leqslant \zeta \leqslant 1$:

$$\partial T(u,\zeta\tau)/\partial\zeta\big|_{\zeta=0,1} = \pm hT(u,\zeta\tau)\big|_{\zeta=0,1}$$
(the "radiation boundary condition") (4)

$$\partial T(\infty,\zeta,\tau)/\partial u = 0 = T(\infty,\zeta,\tau) \tag{5}$$

$$\sqrt{R}E_B(u,0) = E_F(u,0) - \mathcal{J}E_i(u),$$
$$E_B(u,1) = \sqrt{R}E_F(u,1) \tag{6}$$

where $u = r/w$, $\zeta = z/L$, $\tau = t/t_K = Kt/c\rho w^2$, z and r are cylindrical polar co-ordinates, t is time, $\nabla_u^2 = \{\partial/\partial(u\partial/\partial u)\}/u$ assuming radial symmetry, $E_i(u) = (2\mu_o c_o P/\pi w^2)^{1/2}\exp(-u^2)$ =incident amplitude, P = incident laser power, R = reflectance, $\mathcal{J}$ = amplitude transmission coefficient, $H = H_c + H_r$, H_c and H_r being the linearised coefficients for convection and radiation respectively, $T(u,\zeta,\tau)$ =temperature increment above ambient within the sample, with the initial condition $T(u,\zeta,0) = 0$, L = disk thickness, c = specific heat, ρ =density, K = thermal conductivity, $h = HL/K$; $E_F(u,\zeta) = E_{0F}(u,\zeta)\exp(ikn_o - \alpha/2)L\zeta$ and $E_B(u,\zeta) = E_{0B}(u,\zeta)\exp(\alpha/2 - ikn_o)L\zeta$ are the time-independent parts of the light fields of the forward and backward travelling waves within the sample respectively; α =extinction coefficient = $\alpha_a + \alpha_s$, where α_a = absorption coefficient, α_s =scattering coefficient, k = free space wave number = $2\pi/\lambda$, λ =free space wavelength, n_0 = refractive index at $T = 0$; $I_c(u,\zeta,\tau) = (n/\mu_o c_o)|E_F + E_B|^2$, where μ_o and c_o are the vacuum permeability and light speed respectively. We assume the front face of the sample to be at the incident beam waist and take the initial Fabry–Perot detuning to be zero, without loss of generality. $\mathcal{F} = L/kn_o w_o^2$ is the Fresnel number, which gives a measure of the change in beam diameter within the sample due to diffraction. $\mathcal{F}$ is typically less than 0.03 for samples of thickness $\leqslant 1$ mm, whereas $kLn_o \sim 2 \times 10^5$ and $kL(dn/dT)$, which is responsible for the change in beam diameter due to thermal focusing, is about 20. Hence the Laplacian term in Eqs. (2) and (3) constitutes a small perturbation and makes an insignificant contribution to the temperature profile. For a thermo-optic material with a dispersive nonlinearity due to a temperature-dependent refractive index, the optical thickness is

$$nL = n_0 L_0\left[1 + \left\{(dn/dT)/n_0 + (dL/dT)/L_0\right\}T\right] \equiv n_0 L_0(1 + \chi T) \tag{7}$$

where $(dn/\mathrm{d}T)/n_0$ is the thermo-optic coefficient and $(dL/\mathrm{d}T)/L_0$ the linear expansion coefficient. For strongly thermo-optic materials such as PMN and PLZT, $(dn/dT)/n_0$ is an order of magnitude larger[7,10] than $(dL/dT)/L_0$ so we write: $\chi \cong (dn/dT)/n_0$. In this model, we assume that χ and the thermal conductivity K are constant over the temperature range of the experiment. The thermo-optic coefficient is effectively constant over a range of about 20° in the vicinity of the ferroelectric phase transition in relaxor ferroelectrics, such as PMN and PLZT,[10] but exhibits a cusp-like dependence on temperature in displacive transitions.

Solution of Eq. (1) for a steady Gaussian heat source using a Green function in a typical sample disk[16] shows that $T(u, \zeta, \tau)$ is independent of ζ to within 1%. We, therefore, integrate each term in Eq. (1) with respect to ζ to obtain the heat balance equation:

$$\partial^2 T/\partial u^2 + (\partial T/\partial u)/u - \partial T/\partial \tau = (-I_{\text{abs}} + 2HT)w^2/LK \tag{8}$$

where $T(u, \tau)$ now represents temperature averaged over the disk thickness and the absorbed beam intensity is $I_{\text{abs}}(u, \tau) = \int_0^1 \alpha_a I_c(u, \varsigma, \tau) d\varsigma$. Although the transverse Laplacian terms in Eqs. (2) and (3) are essential for determining the diffraction of the laser beam and hence the transmitted beam patterns, the low Fresnel number implies that diffraction is small and, in any case, is opposed by thermal focusing. Hence the *heating effect* of the beam is obtained by neglecting the transverse Laplacian terms, treating u, τ as parameters in the term $n\{T(u, \tau)\}$ and solving Eqs. (2) and (3) with the boundary conditions (5) and (6) for an incident Gaussian beam and integrating to obtain the absorbed irradiance:

$$\begin{aligned} I_{\text{abs}}(u, \tau) &= \frac{\alpha_a I_i(r)(1-R)F_a\left(e^{aL}-1\right)\left(1+R\mathrm{e}^{-aL}\right)}{4\alpha R\left[1+F_a\sin^2\left\{kL(n_0+T(u,\tau)dn/dT)\right\}\right]} \\ &\equiv A(u, \tau) I_i(u) \end{aligned} \tag{9}$$

where $F_\alpha = 4Re^{-\alpha L}/(1 - R\mathrm{e}^{-\alpha L})^2$ is the coefficient of finesse.

3. Thermal focusing oscillations

In the case of negligible finesse (e.g. for BNN and Ce:SBN $F_\alpha \sim 0.01$), Eq. (9) reduces to the time-independent single-pass absorbed intensity:

$$I_{\text{abs}}(u) = I_{\text{i}}(u)(1-R)(1-\mathrm{e}^{-\alpha L})\alpha_a/\alpha \tag{10}$$

where α and α_a may be taken as constant over the relevant temperature range. The system of Eqs. (8) and (10) has been solved by Hankel transformation for both finite and infinite radius samples[15] and by using a Green function[16] to obtain:

$$\begin{aligned} T(u, \tau) = (2P_{\text{abs}}/\pi LK)\int_0^\tau \exp\{-2u^2/(1+8\tau') \\ - \mu^2\tau'\} d\tau'/(1+8\tau') \end{aligned} \tag{11}$$

where $P_{\text{abs}} = 2\pi w^2 \int_0^\infty du' u' I_{\text{abs}}(u') = \left(1 - e^{-aL}\right)\alpha_a \pi w^2 I_p/2\alpha = P\left(1 - \mathrm{e}^{-aL}\right)\alpha_a/\alpha$ is the absorbed power and $\mu^2 = 2w^2 H/LK$. Eq. (11) contains two time-scales: the conduction time scale t_{K}, which determines the establishment of the radial profile for $u \leqslant 1$ and the convection-radiation time scale $t_c = t_K/\mu^2 = \rho cL/2H$ which determines the relaxation time of the whole system to steady state. Setting $u = 0$ in Eq. (11) gives the central sample temperature as a function of time in closed form:

$$\begin{aligned} T(0, 0, \tau) = (P_{\text{abs}}/4\pi LK)\exp(t_K/8t_c) \\ \left[E_1(t_K/8t_c) - E_1\left\{(1+8\tau)t_K/8t_c\right\}\right] \end{aligned} \tag{12}$$

Although Eq. (10) is sufficiently accurate to determine the axially averaged temperature profile and the total transmitted power, it does not contain the phase and amplitude information required to determine the radial profile or the central irradiance of the transmitted and reflected beams. For negligible finesse, the transmitted beam profile is obtained by solving Eq. (2) for $\mathrm{E_F}(u, \zeta)$ using the temperature profile given by Eq. (11). This can either be done numerically by the finite element method or using the analytic solution for Eq. (2).[16] Numerical evaluation shows that the beamwidth of the first transmitted beam decreases by only 10–15% across typical experimental samples. Hence the assumption of a cylindrical Gaussian heat source in Section 2 is self-consistent. By computing the squared modulus of the Fourier transform of the near field transmitted beam $\mathcal{J}E_{\text{F}}(u, L)$ where $\mathcal{J}$ is the amplitude transmission coefficient for light leaving the sample, we obtain the theoretical transmitted and reflected far-field irradiance patterns, which closely match the experimental ones. For example Fig. (2) shows a theoretical plot which closely matches the experimental central intensity transmitted from a Ce:SBN ceramic sample.[3] Following laser switch on, the far field transmitted beam pattern, which is governed by the optical thickness of the sample given by Eq. (7) combined with Eq. (11), evolves from its initial Gaussian shape as the difference in optical thickness $n_o k L_\chi\{T(0, \tau) - T(0.5, \tau)\}$ passes through values $\approx m\pi$ for $m = 1,2,3\ldots$, at which interference between the inner and outer part of the beam causes a succession of central dark spots in the far field pattern surrounded by m bright rings. The plot of central irradiance vs. time shows a minimum for each dark spot separated by a maximum corresponding to a central bright spot. Since Eq. (11) and the interferometric measurements of ref. 15 imply that the temperature profile over the radius of the beam is established within a few times t_K, this is also the time scale of thermal focusing oscillations, e.g. 2–8 ms in the Ce:SBN sample modelled in Fig. (2).

4. Fabry–Perot switching oscillations

As well as giving the temperature evolution in the case of negligible finesse, Eq. (11) represents the *smoothed* solution of Eqs. (8) and (9) for non-negligible finesse obtained by replacing $A(u, \tau)$ by a constant absorption

factor A_s, equal to the average of $A(u, \tau)$ on a time scale large compared to t_K. This smoothed solution has been fitted to the interferometrically measured temperature profile with A_s as an adjustable parameter.[15] To obtain relaxation oscillations, however, we must solve the nonlinear system of Eqs. (8) and (9). This has been done by two methods: (i) numerically by the finite element method for a disk of finite radius and (ii) analytically for a disk of infinite radius.[16] Both solutions show that the central temperature exhibits bistability in the steady state.[7,16] When the laser is rapidly switched to a steady incident power value P, the temperature increases in a stepwise fashion with jumps on a time scale of t_K between metastable states separated by equal increments of central temperature $\Delta T = \pi/kL(dn/dT)$. This gives the characteristic relaxation oscillations in transmitted power and central irradiance shown in Fig. (1) for times much larger than t_K. During the initial few milliseconds, both thermal focusing and Fabry–Perot oscillations occur in these materials, giving a more complicated transient signal. Since the steady-state temperature $T(0, 0, \infty)$ is linearly proportional to P [see Eq. (12)], for low values of P only a few Fabry–Perot oscillations occur, mostly within a time not much larger than t_K. Since the times between these first few oscillations are comparable to t_K, they do not show the quasi-sawtooth pattern of the relaxation oscillations observed over a longer time scale for larger values of P. This was the case for the initial observations of transient oscillations in PLZT[12] but later observations with $P \approx 1$ W have shown relaxation oscillations similar to those observed in PMN.

5. Discussion and conclusions

Transient oscillations under steady illumination, such as those in BNN and Ce:SBN, do not necessarily indicate optical bistability. True optical bistability, i.e. the occurrence of multiple *stable* output states for a single value of incident power above some threshold, is observed in PMN and PLZT, where it arises from thermal bistability due to Fabry–Perot feedback and involves a theoretical S-shaped dependence of temperature on incident power and on time. In transient observations, it is indicated by rapid switching between metastable output values as in Fig. (1). The optical bistability in PMN and PLZT arises from *longitudinal* bistability in the axially averaged temperature profile and that the jumps in the transmitted beam patterns correspond to jumps in the temperature profile over the beam width ("whole beam switching"). Switching waves outside the beam width do not occur. The radially symmetric *transverse* oscillations observed in the far field transmitted and reflected beams are a consequence of relaxation oscillations in the refractive index profile driven by oscillations in the mean internal beam intensity.

References

1. Akhmanov, S. A., Krindach, D. P., Sukhorukov, A. P. and Kohkhlov, R. V., Nonlinear defocusing of laser beams. *JETP Lett*., 1967, **6**, 38–42.
2. Altshuler, G. B., Ermolayev, V. S., Hramov, V. Yu., Zauls, V. and Liberts, G., Self-focusing and self-deflection of laser beams in transparent PLZT ceramics. *Ferroelectr*., 1986, **69**, 67–73.
3. Chen, T., Sheih, S.-J., Scott, J. F. and Chen, H., Temporal dependence of thermal self-focusing in ferroelectric $Ba_2NaNb_5O_{15}$ and Ce^{3+}:$Sr_xBa_{1-x}Nb_2O_6$. *Ferroelectrics*, 1991, **120**, 115–129.
4. Chen, T., Scott, J. F., Sheih, S. J. and Bhalla, A., Optical bistability in ceramic ferroelectrics due to thermal focusing. *Appl. Phys. Lett*., 1992, **60**, 332–334.
5. Chen, T. and Scott, J. F., Thermal focusing and optical bistability in ferroelectrics. *Ferroelectrics*, 1993, **143**, 149–161.
6. Chen, T. and Scott, J. F., Ferroelectric PMN photonic sensors: adiabatic response. *Integ. Ferroelectr*., 1993, **3**, 69–80.
7. Chen, T., Scott, J. F. and Phillipson, P. E., Theoretical models of ferroelectric-photonic sensors. *Integ. Ferroelectr*., 1994, **5**, 1–11.
8. Chen, Z., Shibata, M., Adachi, M. and Kawabata, A., Relaxation oscillations in $PbLa(ZrTi)O_3$ transparent ceramics. *Jpn. J. Appl. Phys*., 1995, **34**, 5396–5400.
9. Firth, W. J., Galbraith, L. and Wright, E. M., Diffusion and diffraction in dispersive optical bistability. *J. Opt. Soc. Am*., 1985, **B2**, 1005–1009.
10. Korshunov, O. Yu., Markovin, P. A. and Pisarev, R. V., Thermooptical study of precursor polarization in ferroelectrics with diffuse phase transition. *Ferroelectr. Lett*., 1992, **13**, 137–142.
11. Krumins, A., Anspoks, A., Odoulov, S. G., Seglins, J. and Vaivods, P., Thermal holograms in doped ferroelectric SBN crystals. *Ferroelectrics*, 1988, **80**, 925–928.
12. Krumins, A., Chen, Z., Shibata, M. and Belov, A. A., Relaxational oscillations in PLZT thermal lenses. *Ferroelectrics*, 1996, **183**, 171–180.
13. Krumins, A., Chen, Z., Ishii, M., Shiosaki, T. and Kawabata, A., Optical bistability in PLZT ceramics due to thermal focusing. *Ferroelectrics*, 1995, **169**, 259–265.
14. O'Sullivan, R. A., Zheng, X., Scott, J. F., Ye, Z. G. and Schmid, H., Aperiodic oscillations in thermal focusing by single crystals of lead magnesium niobate. *Ferroelectrics*, 1996, **186**, 17–20.
15. O'Sullivan, R. A., McGregor, K. W., Cianci, S., Sacca, R., Wilksch, P. A. and Scott, J. F., Temperature profile during spontaneous aperiodic optical bistability oscillations in lead magnesium niobate. *Jpn. J. Appl. Phys*., 1996, **35**, 5203–5209.
16. O'Sullivan, R. A., McGregor, K. W. and Scott J. F., Thermal focusing and optical bistability in ferroelectrics. *J. Phys. Condensed Matter*, in press.
17. Ozolinsh, M., Hanstorp, D. and Lagerwall, S. T., Optical bistability in PLZT ceramics. *Ferroelectrics*, 1997, **201**, 295–304.
18. Scott, J. F. and Chen, T., Optical bistability in lead magnesium niobate ceramics: an integrated photonic flow-rate pressure gauge based upon thermal focusing and convection. *Integ. Ferroelectr*,, 1992, **1**, 71–80.
19. Wright, E. M., Firth, W. J. and Galbraith, I., Beam propagation in a medium with a diffusive Kerr-type nonlinearity. *J. Opt. Soc. Am*., 1985, **B2**, 383–386.
20. Zheng, X., O'Sullivan, R. A. and Scott, J. F., Interpretation of thermally induced optical bistable oscillation. *Integ. Ferroelectr*., 1995, **9**, 225–231.